2026 IEEE/SICE International Symposium on System Integration (SII)
January 11-14, 2026. Cancún, México

Development of the Screw Coupling and the System for Continuous Evaluation of Connection Mechanism

Tasuku Makabe, Naoya Yamaguchi, Iori Yanokura, and Kei Okada

***Abstract*— Multiple modular robots use attachment/detachment couplings to adapt to diverse tasks and environments. Sharing the same physical components across different robots and applications requires couplings that (1) have low backlash, (2) are low cost, and (3) allow easy attachment and detachment. However, the presence of multiple couplings on a robot makes it challenging to maintain reliable mechanical and electrical connections. We propose a 3D-printable screw-type electromechanical coupling (“Screw Coupling”), demonstrate its integration into heterogeneous components, and present applications on multiple robots. We also introduce a system that continuously applies loads and moments to the coupling during operation, enabling real-time evaluation and ensuring long-term reliability.**

I. INTRODUCTION

Modular robots that can reconfigure their morphology according to task and environment [1] have been applied to locomotion, manipulation, and environment-adaptive structures [2], [3]. Couplings include motor-driven locking pawls [4], magnetic-mechanical hybrids [5], and simple hand-operated fasteners [3].

To scale the number of components in a robot system and realize diverse morphologies while maintaining the required motion performance for practical tasks, the coupling should provide:

1) Low backlash
2) Low manufacturing cost
3) Easy attachment and detachment
4) Testing Connection Mechanism

We propose a screw-type attachment/detachment coupling (“Screw Coupling”) that combines (1) low backlash and (3) ease of operation, and is (2) manufacturable via low-cost laboratory 3D-printing. While 3D-printed parts are easily fabricated, they often suffer from dimensional variability due to printing conditions, unlike parts produced by machining or injection molding. This variability is critical for couplings that demand high uniformity and reliability. To address this, we present (4) a system for continuous evaluation of mechanical strength and communication functionality during robot operation, enabling couplings that meet the above requirements and maintain performance across diverse applications.

II. RELATED WORK AND OUR CONTRIBUTION.

A. Related Work

Modular reconfigurable robots (MRR) have long been studied as systems that adapt to diverse morphologies and environments [6]; here, we focus on the interface between

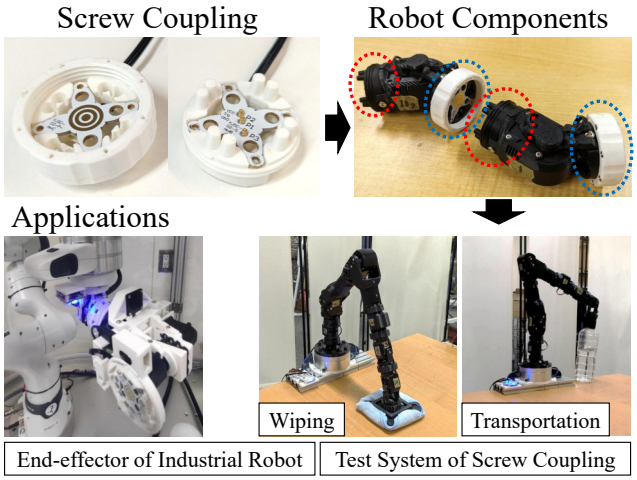

Fig. 1: Screw Coupling and Robot Components Separated by Couplings and Applications.

modules—the attachment/detachment coupling [7]. Modules connect through the coupling at three distinct levels:

- Level 1: Mechanical connection
- Level 2: Communication (data) connection
- Level 3: Power connection

Level 1 is a mechanical connection for forming a continuous body. Examples include claw or screw-thread mechanisms [8], designs exploiting material changes from temperature or chemical reactions [9], and couplings using permanent or electromagnets [10]. The choice depends on the required joint strength and ease of operation. Level 2 is a communication connection for data exchange between modules. Wired implementations often use electrical contacts such as pogo pins, while wireless ones typically employ short-range infrared (IR). Level 3 is a power connection for sharing energy between modules. Although each module usually carries its own battery, some systems —e.g., spherical robots—use a conductive outer shell as a terminal to balance battery charge and enhance redundancy [11].

Multiple connection levels can be combined to meet task needs, but adding functions increases per-module components, weight, volume, and cost. A larger number of couplings in the system also reduces overall performance. We therefore propose a simple screw coupling that implements only the essential functions across the three levels. 3D-printing, widely used in both conventional robotics [12] and soft robotics [13], [14], enables easy fabrication but

978-1-6654-5784-2/26/$31.00 ©2026 IEEE

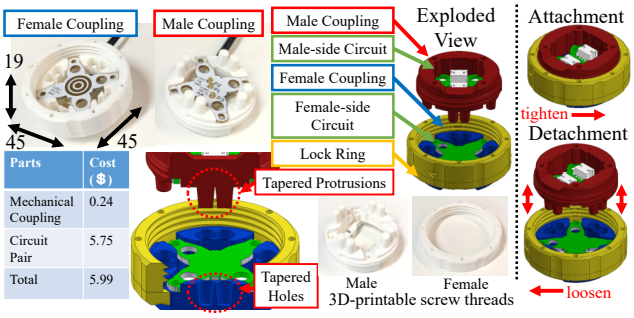

Fig. 2: Design of Screw Coupling

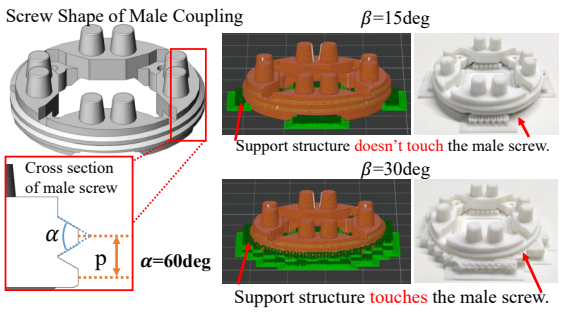

Fig. 3: 3D-printing method of Screw Coupling

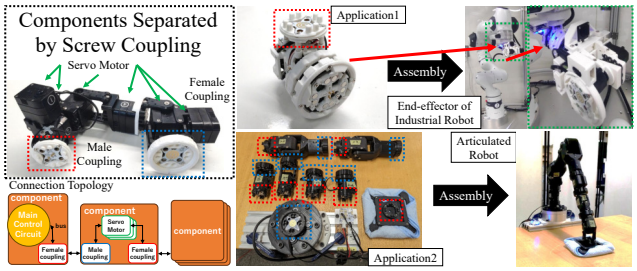

Fig. 4: Separated Robotic Components by Electromechanical Couplings

suffers from geometric variability. To address the resulting reliability concerns, we also present a system that allows module-level part replacement and continuous evaluation of mechanical strength and communication performance during robot operation.

B. Our Contribution

Our contributions are threefold:

1) We present a structure that minimizes backlash by combining a screw with tapered male/female features.
2) We design the geometry to be easily mass-produced by 3D-printing.
3) We propose a system for continuous reliability evaluation of the coupling.

To minimize backlash, relative positions among structures must be constrained by an alignment geometry and a sustained normal force on that geometry. In our design, the screw acts elastically to generate axial preload that continuously pulls the tapered faces together, thereby reducing backlash. Regarding 3D-printability, unlike prior hand-locking designs [3], our geometry is manufacturable even with commodity FDM printers, enabling rapid composition of diverse components. Finally, because 3D-printed parts exhibit dimensional variation, a system that continuously evaluates the reliability of assembled couplings is indispensable.

III. Design of 3D-printable Screw Coupling

The couplings shown in Fig.2 consists of a fastening mechanism that can be fabricated using a low-cost, commercially available 3D-printer [15], and an electronic circuit equipped with pogo pins and pads. Both the mechanical and electrical components can be manufactured using mass-production-friendly methods, and the mechanism can be fabricated at the cost indicated in Fig.2. The male side comprises a circuit board with concentric pads and an outer housing with a male screw, while the female side consists of a circuit board with pogo pins and an outer housing incorporating a retaining ring with an internal female screw. This configuration enables simultaneous mechanical and electrical attachment/detachment. By applying axial force through the threaded structure, the mechanism minimizes backlash when drawing together and securing the male and female parts—featuring a tapered protrusion on one side and a corresponding tapered hole on the other.

A. Design of 3D-printable Screw Shape

As shown in Fig.3, the mechanism uses external (male) and internal (female) screw structures fabricated with a standard FDM-type 3D-printer. Threaded geometries can be printed either by adding and later removing support material, or by designing them to avoid support altogether. Here, the screw geometry was custom-designed with a low-overhang profile to eliminate support, allowing dimensions such as pitch p and thread angle α to be freely specified. Most slicers define an "overhang threshold angle" β, above which support is automatically generated; to avoid adhesion on the threads, the slope must be less than β (eqn: eq1). Fig.3 compares supported and support-free cases; in this study, β was set to 15 $[deg]$.

$$\alpha/2 > \beta \tag{1}$$

B. Applications of Screw Coupling

Fig.4 illustrates application examples of the proposed coupling. In this study, servo motors and sensors compatible with three-wire half-duplex UART communication, including power lines, were used. In Application Example 1, the proposed mechanism is mounted at the end of an existing robotic arm, with a common control board installed on the arm side, enabling rapid exchange of end-effectors according to task requirements. In Application Example 2, multiple types of components are equipped with a pair of male/female attachment/detachment interfaces, allowing the assembly of multi-joint manipulators through various component combinations.

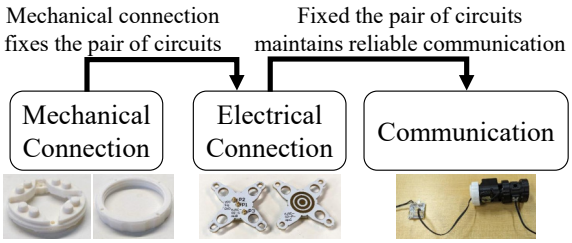

Fig. 5: Dependencies Between

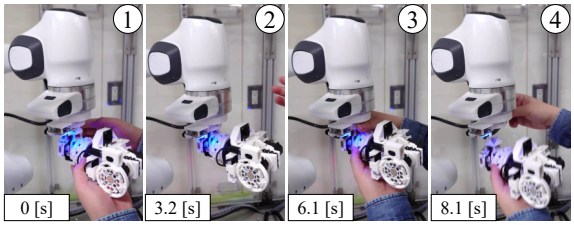

Attachment: 3.2 [s] Detachment: 2.0 [s]

Fig. 6: Evaluation of Operation Time of Coupling

IV. Testing System for Connection Mechanism of Screw Coupling

In this section, we examine the evaluation items and their corresponding evaluation methods in order to develop a continuous evaluation system for the connection functions provided by the coupling. Subsequently, we conduct evaluations corresponding to the aforementioned evaluation criteria to validate the proposed couplings.

A. Dependencies between Connection Mechanisms to be Evaluated

From the perspective of evaluating the robustness and reliability of the coupling, the evaluation items can be classified into the following three categories:

1) Mechanical connection: Whether it can withstand external loads without breakage and loosening.
2) Electrical connection: Whether good contact between terminals can be maintained.
3) Communication connection: Whether communication quality can be continuously maintained.

These connection functions have the dependency relationship shown in Fig.5. Specifically, maintaining the mechanical connection preserves the physical contact between circuit boards, thereby maintaining the electrical connection. Maintaining the electrical connection, in turn, ensures continuous communication, which sustains the communication connection. Therefore, when evaluating a given connection function, it is also necessary to evaluate the higher-level dependent connection functions simultaneously.

Furthermore, the evaluation items include those that can be assessed using discrete values, such as mechanical breakage or communication loss, and those that can be assessed using continuous values, such as deflection, communication quality, or loosening amount. The former represent strict constraints—conditions that must always be satisfied to meet the intended functionality—whereas the latter represent looser constraints, where the goal is to optimize the continuous values.

B. Evaluation of Mechanical Connection

1) Overview of Mechanical Connection Evaluation: In evaluating the mechanical connection, it is necessary to determine whether the coupling can withstand the loads and vibrations encountered during robot operation without breaking, deforming excessively, or loosening. As an evaluation method, the load applied to the mechanism alone can be measured using a six-axis force/torque sensor while either an operator applies external forces or the robot executes autonomous movements, thereby maintaining a condition in which time-varying six-axis loads are continuously applied to the mechanism. In addition, we measured the manipulation time of coupling to evaluate simplicity.

2) Evaluation of Manipulation Time of Screw Couplings: Fig.6 shows the experimental setup used to measure the time required for attachment and detachment operations.

The attachment operation was performed according to the following steps:

1) Insert the tapered protrusion of the male mechanism slightly into the tapered hole of the female mechanism.
2) While pressing the two mechanisms together, rotate until the retaining ring engages.
3) Rotate the retaining ring in the tightening direction until it can no longer be turned by hand.

The detachment operation was performed as follows:

1) Rotate the retaining ring in the loosening direction.
2) Once the retaining ring disengages from the male mechanism, pull the male mechanism out from the female mechanism.

The results show that the attachment operation can be completed in approximately 3.2 [s], while the detachment operation requires approximately 2.0 [s], confirming that detachment can be performed in a shorter time.

C. Evaluation of Electrical Connection

1) Overview of Electrical Connection Evaluation: In evaluating the electrical connection, it is necessary to verify whether the circuit boards equipped with pogo pins and pads are fixed in the intended relative position by the mechanical connection, and whether this state is maintained. As an evaluation method, to confirm that the terminals are connected as designed, continuity measurements are performed to check whether the required terminals are conducting and whether terminals that should not be connected remain isolated. This corresponds to an evaluation using discrete values. In this study, the mechanism was evaluated by connecting a servo motor through the attachment/detachment interface and confirming whether the intended operation could be sustained.

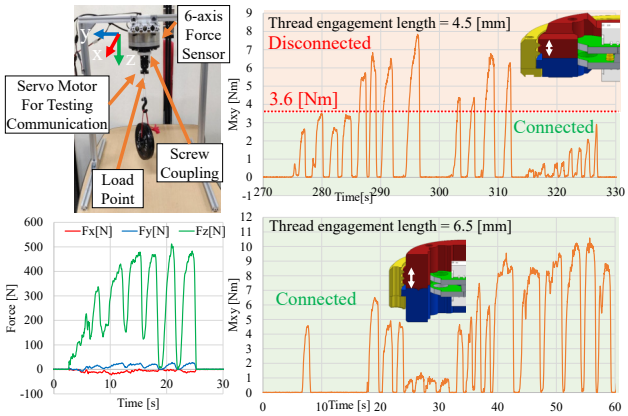

Fig. 7: Evaluation of Communication Rigidity

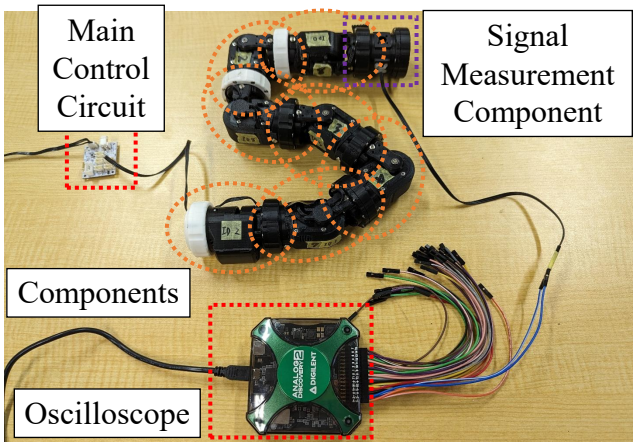

Fig. 8: Evaluation of Signal Shape

2) Evaluation of Communication under External Torque: Fig.7 shows the results of evaluating the ability of the coupling to maintain communication under load. In this evaluation, the engagement length of the threaded section was set to two values 4.5 [mm] and 6.5 [mm] and both the mechanical strength and the communication retention performance under load were compared. Increasing the engagement length enhances clamping force and thus mechanical strength; however, it also entails a trade-off in the form of increased size and weight.

For mechanical strength, with an engagement length of 4.5 [mm], the mechanism weighed 18 [g] and was able to withstand at least 50 [kg] of tensile load. Regarding communication performance, with the 4.5 [mm] engagement length, communication was maintained up to approximately 3.6 [Nm] of applied torque, as shown in the results. Since such loads can easily occur in applications like the robotic arm described later, this strength was deemed insufficient.

When the engagement length was increased to 6.5 [mm], communication was maintained up to approximately 10.5 [Nm] of applied torque, representing at least a three-fold improvement in load tolerance, as confirmed by the results.

D. Evaluation of Communication

1) Overview of Communication Evaluation: In evaluating the communication connection, it is necessary to determine whether the communication signal waveform changes when transmitted through the coupling, whether communication can be sustained under such conditions, and how communication quality—such as signal waveform characteristics—changes. Possible evaluation methods include a discrete-value evaluation to verify whether communication between multiple devices (e.g., between the control board and a servo motor) is maintained, and a continuous-value evaluation to measure changes in signal waveform that depend on the number of attachment/detachment interfaces in the path.

In general, there is a trade-off between signal waveform quality (rise and fall times) and communication baud rate. Therefore, in this study, communication connection performance was evaluated based on whether communication could be established with commercially available serial servos (TTL, up to 1.25 [Mbps]). Furthermore, in an environment where multiple servo motors share the same communication line, the effect of the number of connected components on waveform characteristics was measured and evaluated while varying the communication baud rate.

2) Evaluation of Signal Quality: Fig.8 presents the results of evaluating the communication robustness of a robot equipped with the proposed coupling. In this evaluation, the number of connected components was varied from one to seven, and two communication speeds 1.25 [Mbps] and 625 [kbps] were tested to determine whether communication could be maintained. As shown in the figure, the signal waveform was measured by inserting an intermediate component that allows the signal line to be tapped.

The results indicate that as the number of components increases, the rise time of the half-duplex (open-drain) signal line becomes longer. At 1.25 [Mbps], communication became unstable when the number of components exceeded five, whereas at 625 [kbps], stable communication was maintained with up to seven components.

Consequently, in the evaluation of the six-degree-of-freedom manipulator described later, the communication system was configured entirely at 625 [kbps]. While this phenomenon also occurs with conventional pogo pin contacts, it is more pronounced in the proposed method, in which multiple pogo pin and pad pairs are implemented within the same communication line. This makes the finding an important consideration for practical implementation.

V. Evaluation System of Screw Couplings and Experiments

Using the proposed coupling, which was evaluated independently in this study, we constructed the multi-joint

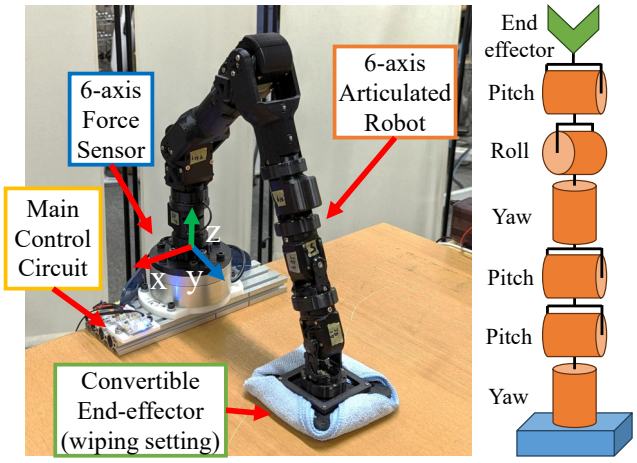

Fig. 9: Overview of Evaluation System

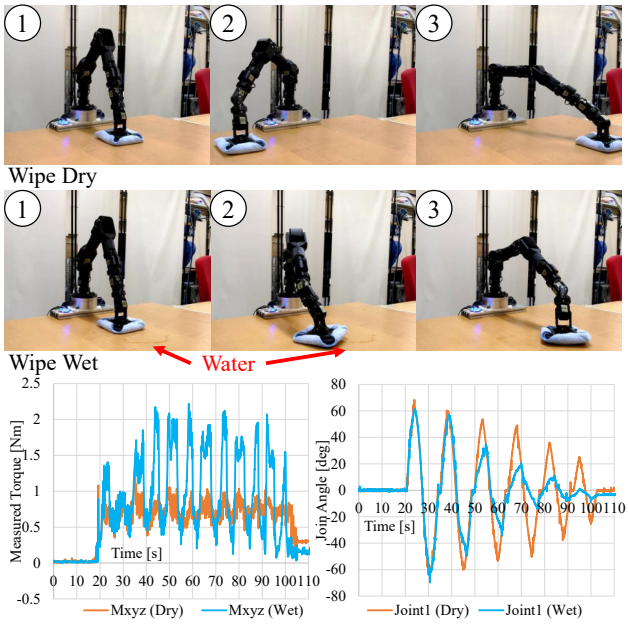

Fig. 10: Experiment of Wiping Motion

arm system shown in Fig.9. The system is equipped at its base with a six-axis force/torque sensor fixed to the female side of the coupling, and consists of six interconnected components, each containing a servo motor and one male-female pair of the coupling. A female-side coupling is also installed at the end of the arm, allowing the end-effector to be replaced. This configuration enables verification of whether the system can operate while subjected to internal forces caused by environmental contact and external forces from applied loads. In this section, internal forces were applied by performing a desk-wiping motion with a cloth, while external forces were applied by continuously moving a weight, and the system was evaluated under these conditions.

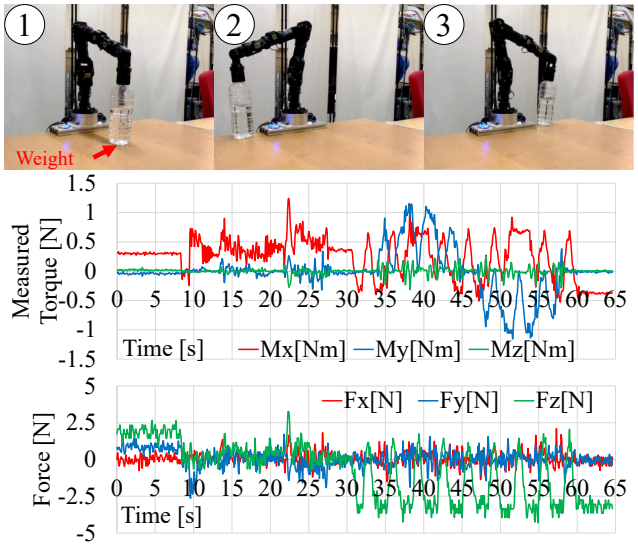

Fig. 11: Experiment of Transportation Motion

A. *Wiping Task Experiment*

Fig.10 shows an overview and evaluation results of the desk-wiping task. In the dry-wiping experiment, the system initially operated stably while storing internal forces; however, after approximately 10 minutes of operation, the tracking performance of the base yaw-axis servo deteriorated, preventing continuous wiping motion. At that time, the six-axis force/torque sensor recorded maximum combined values of 12.4 [N] in moment and 4.2 [N] in load (each combined across three axes). While moment is the factor most strongly affecting communication performance, these values were confirmed to be sufficiently smaller than the previously measured 10.5 [Nm]. When water was applied to the desk and wiping was performed, the motion itself could still be executed; however, as the cloth absorbed water, the frictional force with the environment increased, and the tracking performance of the base yaw axis of the six-axis arm was notably reduced. Through these experiments, it was found that the connection performance of the coupling was sufficient to generate the pressing force required for wiping tasks, but reducing internal forces is necessary to ensure sustained operation.

B. *Transportation Task Experiment*

Fig.11 presents an overview and evaluation results of the continuous weight-transport experiment. In this experiment, a weight of 393 [g] was attached to the tip of the arm to apply an external load, and the arm repeatedly lifted and placed the weight from and onto the desk to evaluate its ability to sustain operation. As shown in the results, the system was able to operate continuously for up to approximately 10,000 seconds. During this period, the maximum load and moment experienced were approximately 4.5 [N] and 1.47 [Nm], respectively. Furthermore, communication functionality was maintained throughout the experiment, confirming that the connection performance of the coupling was sufficient.

VI. Discussion

The performance evaluations highlight the operational characteristics and limitations of the proposed screw coupling in practical scenarios. Attachment and detachment were executed in approximately 3.2 [s] and 2.0 [s], respectively, owing to the screw structure and tapered geometry that facilitate rapid alignment and secure fastening. Communication stability was found to depend on the number of connected components; instability arose beyond five connections at 1.25 [Mbps], primarily due to increased electrical resistance and parasitic capacitance. Mechanical strength tests revealed that increasing the thread engagement length from 4.5 [mm] to 6.5 [mm] significantly enhanced torque tolerance (from 3.6 [Nm] to 10.5 [Nm]), underscoring the influence of geometric parameters on coupling rigidity. Task-based experiments demonstrated adequate load-bearing capacity; however, the wiping task induced servo performance degradation over extended operation due to friction and water absorption effects, whereas the transportation task maintained stable operation for 10000 [s] under moderate loads, with only minor positional deviations caused by coupling and frame deflection. These observations indicate that coupling performance alone does not dictate long-term reliability; the surrounding mechanical structure and actuation components play an equally critical role in sustaining operational stability under demanding conditions.

Furthermore, we explore methods to extend the limitations identified in this paper and the insights gained from them to the continuous evaluation of diverse modular robots. In the robot system presented in this paper, a single top-level control board connects a single internal communication system to numerous detachable mechanisms. Consequently, communication failures in one part can affect the entire system. Therefore, in typical modular robots where each individual robot possesses its own control board, it becomes possible to observe connection status redundantly from multiple control boards. Furthermore, while the current evaluation was conducted on pre-assembled robots, applying this to robots that actively perform docking and undocking requires updating the communication system before and after docking/undocking. Consequently, evaluating the success rate of communication restoration itself should also be added as an assessment item.

VII. Conclusion

We developed a 3D-printable screw coupling and demonstrated its integration into multiple robotic components. For the targeted size and applications, the coupling met key requirements, supporting loads over 2000 times its own weight and maintaining communication under torques up to 10.5 [Nm]. We built continuous evaluation system, enabling multi-hour monitoring of mechanical strength and communication performance under both internal and external forces.

This study primarily focuses on the mechanical structure of the coupling mechanism and the configuration of a continuous evaluation system for evaluating coupling performance. Future work includes establishing a generalized design theory for low-backlash connectors by developing a mechanical model of the coupling and clarifying design guidelines—such as the optimal taper angle—based on that analysis. Moreover, the proposed continuous evaluation framework could be extended to evaluate other types of existing couplings and to diagnose multiple failure modes, further enhancing its applicability and generality.

References

[1] T. Fukuda, T. Ueyama, Y. Kawauchi, and F. Arai, "Concept of cellular robotic system (cebot) and basic strategies for its realization," *Computers & electrical engineering*, vol. 18, no. 1, pp. 11–39, 1992.

[2] F. Negrello, M. Garabini, M. G. Catalano, J. Malzahn, D. G. Caldwell, A. Bicchi, and N. G. Tsagarakis, "A modular compliant actuator for emerging high performance and fall-resilient humanoids," in *Humanoids2015*. IEEE, 2015, pp. 414–420.

[3] A. Yun, D. Moon, J. Ha, S. Kang, and W. Lee, "Modman: an advanced reconfigurable manipulator system with genderless connector and automatic kinematic modeling algorithm," *IEEE Robotics and Automation Letters*, vol. 5, no. 3, pp. 4225–4232, 2020.

[4] A. Spröwitz, R. Moeckel, M. Vespignani, S. Bonardi, and A. J. Ijspeert, "Roombots: A hardware perspective on 3d self-reconfiguration and locomotion with a homogeneous modular robot," *Robotics and Autonomous Systems*, vol. 62, no. 7, pp. 1016–1033, 2014.

[5] T. Makabe, K. Okada, and M. Inaba, "Development of the Assembling System for Structure Transformable Humanoid with Attach-Lock-Detachable Magnetic Coupling (in press)," in *Proceedings of The 2024 IEEE International Conference on Robotics and Automation*. IEEE, 2024.

[6] G. Liang, D. Wu, Y. Tu, and T. L. Lam, "Decoding modular reconfigurable robots: A survey on mechanisms and design," *The International Journal of Robotics Research*, vol. 44, no. 5, pp. 740–767, 2025.

[7] W. Saab, P. Racioppo, and P. Ben-Tzvi, "A review of coupling mechanism designs for modular reconfigurable robots," *Robotica*, vol. 37, no. 2, pp. 378–403, 2019.

[8] S. Murata, E. Yoshida, A. Kamimura, H. Kurokawa, K. Tomita, and S. Kokaji, "M-tran: Self-reconfigurable modular robotic system," *IEEE/ASME transactions on mechatronics*, vol. 7, no. 4, pp. 431–441, 2002.

[9] P. Swissler and M. Rubenstein, "Fireant3d: a 3d self-climbing robot towards non-latticed robotic self-assembly," in *2020 IEEE/RSJ International Conference on Intelligent Robots and Systems (IROS2016)*. IEEE, 2020, pp. 3340–3347.

[10] C. Liu, Q. Lin, H. Kim, and M. Yim, "Smores-ep, a modular robot with parallel self-assembly," *Autonomous Robots*, vol. 47, no. 2, pp. 211–228, 2023.

[11] G. Liang, Y. Tu, L. Zong, J. Chen, and T. L. Lam, "Energy sharing mechanism for a freeform robotic system-freebot," in *Proceedings of The 2022 IEEE International Conference on Robotics and Automation*. IEEE, 2022, pp. 4232–4238.

[12] T. Makabe, T. Himeno, K. Okada, and M. Inaba, "Development and application of the low-cost 3d printable servo module with the worm gear reduction mechanism capable of switching between open and driven states," in *SII25*. IEEE, 2025, pp. 1235–1240.

[13] T. Wallin, J. Pikul, and R. F. Shepherd, "3d printing of soft robotic systems," *Nature Reviews Materials*, vol. 3, no. 6, pp. 84–100, 2018.

[14] S. Yoshimura, A. Miki, K. Miyama, Y. Sahara, K. Kawaharazuka, K. Okada, and M. Inaba, "Patterned structure muscle: Arbitrary shaped wire-driven artificial muscle utilizing anisotropic flexible structure for musculoskeletal robots," in *IROS2024*. IEEE, 2024, pp. 13 930–13 937.

[15] "Bambu Lab X1-Carbon 3D Printer(Bambu Lab)." https://us.store.bambulab.com/products/x1-carbon.